

Current-Induced Magnetization Reversal in High Magnetic Fields in Co/Cu/Co Nanopillars

B. Oezylmaz and A. D. Kent

Department of Physics, New York University, New York, NY 10003, USA

D. Monsma

Department of Physics, Harvard University, Cambridge, MA 02143, USA

J. Z. Sun, M. J. Rooks and R. H. Koch

IBM T. J. Watson Research Center, P.O. Box 218, Yorktown Heights, NY 10598, USA

(Dated: 12/16/02)

Current-induced magnetization dynamics in Co/Cu/Co trilayer nanopillars ($\sim 100\text{nm}$ in diameter) has been studied experimentally for large applied fields perpendicular to the layers. An abrupt and hysteretic increase in dynamic resistance is observed at high current densities for one polarity of the current, comparable to the giant magnetoresistance effect observed at low fields. A micromagnetic model, that includes a spin-transfer torque, suggests that the current induces a complete reversal of the thin Co layer to alignment antiparallel to the applied field—that is, to a state of maximum magnetic energy.

PACS numbers: 75.60.Jk, 75.75.+a, 75.30.Ds

Angular momentum transfer in magnetic nanostructures mediated by an electric current has become the subject of intense research. Sloncszewski and Berger first considered this theoretically in 1996 [1, 2]. Its experimental observation a few years later [3, 4, 5, 6, 7] has boosted efforts to understand the influence of the conduction electron spin on the magnetization dynamics of ferromagnetic nanostructures in the presence of high electric currents. A spin current has been demonstrated to switch the magnetization direction of a small magnetic element. Reversible changes in multilayer resistance have also been observed and associated with magnetic excitations or the generation of spin-waves. However, an in-depth understanding of the relationship between these two phenomena—reversible excitations of the magnetization and irreversible switching of the magnetization—is still missing.

In the initial experiments a point-contact was employed to inject high current densities into a magnetic multilayer [3, 6, 7]. Subsequent experiments have concentrated on the reduction of the lateral size of Co/Cu/Co trilayers to the sub-micron scale, resulting in the fabrication of nanopillar devices [8, 9, 10, 11, 12, 13, 14]. In the point-contact experiments the applied magnetic field was oriented perpendicular to the thin film plane and was larger than the film demagnetization fields ($H \geq 2$ T). In this high field regime a peak structure in the dynamic resistance (dV/dI) at a critical current was interpreted as the onset of current induced excitation of spin-waves in which the current induced spin-transfer torque leads to the uniform precession of the magnetization [3, 6, 15]. Spin-transfer torque studies on pillar devices concentrated on magnetic fields applied in the thin film plane. In the low-field regime, a hysteretic jump in the dynamic resistance was observed; clear evidence for current induced magnetization reversal of one of the mag-

netic layers [8, 9, 10, 11, 12, 13, 14]. Hence, the effect of the spin-polarized current on the magnetization seemed to be quite distinct in the low and high field regime. Experimentally, a current induced hysteretic magnetization reversal was only observed at low fields in nanopillar devices.

In this letter we report detailed studies of current induced dynamics of the magnetization in sub-micron size pillar devices at high magnetic fields in the field-perpendicular to the plane geometry. For sufficiently large currents of one polarity hysteretic magnetic switching of the layers is observed at high magnetic fields. In contrast to previous results in this geometry with mechanical point contacts, these results cannot be understood as small amplitude excitations of the magnetization. Micromagnetic modeling suggests that spin-transfer torques induce precessional states which evolve into a static state of anti-parallel alignment of the layers.

Sub-micron size pillar devices with the stack sequence of $|\text{3nm Co}|10\text{nm Cu}|12\text{nm Co}|300\text{nm Cu}|10\text{nm Pt}|$ were fabricated by thermal and electron-beam evaporation through a sub-micron stencil mask [13]. The thin Co-layer has a lower coercivity and is the “free” layer in the device. The thick Co-layer is magnetically hard and hence is relatively insensitive to the current induced torque. It is the “fixed” layer in the device and acts to setup a spin-polarized current in the intervening Cu layer. The inset in Fig. 1a shows a sketch of the pillar device. Details of fabrication and transport properties at low in-plane fields can be found elsewhere [14]. Many junctions were studied thoroughly as a function of current and applied magnetic field. In this paper, we discuss representative data obtained on a sample of lateral size $90\text{ nm} \times 140\text{ nm}$. All transport measurements reported here were conducted at 4.2 K. The dynamic resistance dV/dI was measured by means of phase-sensitive lock-in

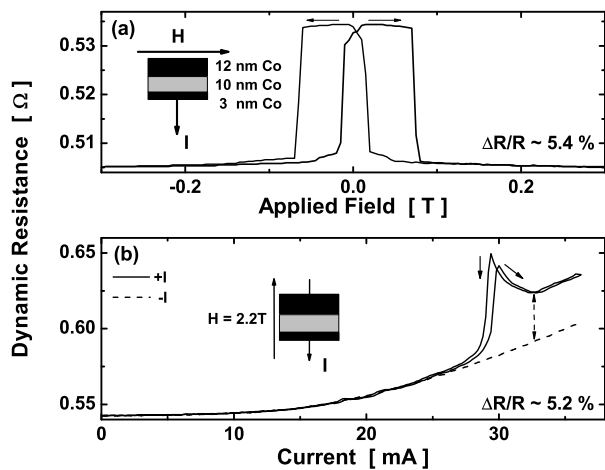


FIG. 1: (a) dV/dI versus H for fields oriented in the plane of the thin-film layer and small bias currents. The inset shows the layers sequence. (b) dV/dI versus I of the same device. The applied field is $H=2.2$ T and oriented perpendicular to the film plane. At a critical current a peak structure occurs in the dynamic resistance. The dotted line shows dV/dI at negative currents, for which the peak structure is absent.

technique with a $100 \mu\text{A}$ modulation current at $f=800$ Hz added to a dc bias current. The dc voltage was recorded simultaneously. We define positive bias such that the electrons flow from the free layer to the static layer.

A typical magnetoresistance (MR) measurement of our pillar devices at 4.2 K with an applied field in the plane of the thin films is shown in Fig. 1a. The device exhibits a clean transition between a low resistance and high resistance state corresponding to parallel (P) and anti-parallel alignment (AP) of the magnetization of the two Co-layers. At 4.2 K the MR of this sample is 5.4 %. Due to magnetostatic interactions between the layers, the high resistance state is reached before the sign of H is reversed[8, 12]. Fig. 1b shows dV/dI versus I with the applied field perpendicular to the film. Here the applied field ($H=2.2$ T) is larger than the demagnetization field of Co thin films ($4\pi M \approx 1.5$ T). The sweep to negative currents is shown as the dashed line in the figure. From the data it is evident that the abrupt change in resistance occurs only for one current direction. In addition, the onset of this change in resistance is sharp and takes place at a critical current, I_c . Its characteristic signature is a peak structure in the dynamic resistance measurements. In the simultaneous dc-measurement (not shown) this feature corresponds to a step-like increase of the dc-voltage. There is also a parabolic increase in the background resistance for both directions of the current due to increased electron scattering at high current densities.

In earlier reports the peak structure in the dynamic

resistance of point contacts was attributed to the excitation of a uniform precession of the free layer [3, 6, 15]. However, this picture cannot explain our data. First, the resistance change is large. This can be seen by either looking at the change of slope in the dc-voltage at the critical current I_c or by comparing the dynamic resistance for I greater than I_c with the dynamic resistance at the same current value but with opposite polarity at which the abrupt change in resistance is absent. Either comparison shows a change in resistance of about 5 % similar to the GMR value of the same device (Fig. 1a). Therefore, an explanation in terms of a small deviation of the free layer magnetization from its parallel alignment with respect to the static layer is not sufficient to explain the observed resistance change. With the measurement of a resistance change comparable to the GMR effect, it seems plausible to assume that even at high fields the spin transfer effect can produce a full reversal of the magnetization. Second, the change in device resistance is hysteretic, occurring at higher current density for increasing current (Fig. 1b). The excitations of spin-waves would decay rapidly on the time scale of such measurements and thus appear reversible in such I-V measurements. Further, as we show below, this interpretation is consistent with micromagnetic modeling.

The magnetic field dependence of the critical current is summarized in the gray-scale plot of Fig. 2a. Here the current is swept up from 20 mA to 36 mA while the magnetic field is held constant for each current sweep. For subsequent current sweeps the field is raised from 0.34 T to 2.7 T in steps of 5 mT. In this gray-scale plot a critical current I_c separates the “applied field-current bias” plane into two regions. Below the critical current the device remains in its low resistance state, in which both layers are in the parallel orientation. Above the critical current, the magnetization of the device is in a higher resistance state, in which the relative orientation of the magnetization of the two layers deviates strongly from a parallel configuration.

The critical current for decreasing current is shown as the dashed line in this figure. Looking at the field dependence of the hysteresis ΔI_c and the field dependence of the critical current I_c , one can distinguish two regions. Above 1.4 T the critical current increases with applied magnetic field. In this region also ΔI_c generally increases with increasing field. (There is a deviation from this behavior between 2.0 T and 2.4 T, in which ΔI_c actually decreases.) However, below 1.2 T the critical current decreases linearly with applied magnetic field. In this field region (1.1 T \rightarrow 0.35 T), the hysteresis is near the limit of our experimental resolution. The resistance jumps for both regions are similar in magnitude, i.e. close to the GMR value. To understand these results we consider the Landau-Lifshitz-Gilbert (LLG) equations of motion for the free layer including a spin-current induced torque predicted by Slonczewski [1, 15]:

$$\frac{d\hat{m}}{\gamma dt} = -\hat{m} \times [\vec{H}_{eff} - \alpha \frac{d\hat{m}}{\gamma dt}] + a_I \hat{m} \times (\hat{m} \times \hat{m}_P) \quad (1)$$

FIG. 2: (a) Magnetic field dependence of dV/dI versus I . The gray scale represents the dynamic resistance of the junction. Light color corresponds to high resistance and dark to low resistance. The dashed line shows the position of the jump in resistance for down-sweep of the bias current. (b) Micro-magnetic simulations of the experiment as described in the text.

To simplify the analysis we assume that the magnetic layers behave as single domains, so that \hat{m} and \hat{m}_P are unit vector in the direction of the magnetization of the free and fixed layer respectively. \vec{H}_{eff} is the effective field, $\vec{H}_{eff} = \vec{H} - 4\pi M(\hat{m} \cdot \hat{z})\hat{z}$, where \vec{H} is the applied external field, \hat{z} is the film normal and $4\pi M = 1.5T$ for Co. γ is the gyromagnetic ratio. The second term in the brackets is the damping term and α is the Gilbert damping parameter ($\alpha \ll 1$). The last term incorporates the spin-transfer effects. The prefactor, a_I , depends on the current, the spin-polarization of the current P and the angle between the free and pinned magnetic layers Θ , $a_I = \frac{\hbar I}{eMV}g(P, \Theta)$ [1]. Here g is a function of the polarization P that increases with Θ and V is the volume of magnetic element. An increase in a_I with angle has been found in a number of different approaches to modeling the spin-transfer effect [16, 17, 18, 19].

In the large field regime ($H > 4\pi M$) the equation of motion can be simplified. Initially both layers are parallel to the applied field and the z-component of the free layer magnetization satisfies (neglecting terms of order α^2):

$$\frac{dm_z}{\gamma dt} = (1 - m_z^2)[\alpha(H - 4\pi M m_z) - a_I] \quad (2)$$

From this equation it can be seen that an initial state $m_z = 1$ aligned with the applied field in the z direction will become unstable when $a_I > \alpha(H - 4\pi M m_z)$. States for which $|m_z| < 1$ and $\frac{dm_z}{dt} = 0$ correspond to precession of the magnetization in the x-y plane at angular frequency of about $\gamma(H - 4\pi M m_z)$. Importantly, note that a solution with magnetization antiparallel to the effective field ($m_z = -1$) occurs for $a_I > \alpha(H - 4\pi M)$ and corresponds to a static magnetization ($\frac{dm_z}{dt} = 0$). Thus the spin-torque, in this case, leads to a state of maximum magnetic energy of the free layer. Similar high energy states have also been observed in numerical studies for the field in-plane geometry [20, 21]. As a_I increases with Θ the transition between a precessing state with $|m_z| < 1$ and $m_z = -1$ occurs rapidly with increasing current and is hysteretic. For example, hysteresis occurs when, $a_I > \alpha(H + 4\pi M)$ for $\hat{m} \cdot \hat{m}_P = -1$ while at the same current $a_I < \alpha(H - 4\pi M)$ when $\hat{m} \cdot \hat{m}_P = 1$. In addition, for increasing applied field, the transition occurs at higher current and the width of the hysteresis increases.

Fig. 2b shows the result of integration of the eqn. 1 under the conditions approximating the experiment

($P = 0.4$ for Co and $\alpha = 0.007$). The device resistance is plotted on a gray scale versus I and H and is computed from the angle between the fixed and free layers using the analytic expression: $R = (1 - \cos^2(\theta/2))/(1 + \cos^2(\theta/2))$ [16, 19, 22]. For $H < 4\pi M$ (below the horizontal dashed line in the figure) the pinned layer magnetization tilts into the plane and thus the pinned layer and effective field are no longer collinear. In this case, we find precessional states of the magnetization, with the projection of \hat{m} on \hat{m}_P decreasing with increasing current. The average resistance is plotted below this line. The dashed-dotted line shows the transition to a lower resistance state for decreasing currents, i.e., for states starting with the layers initially anti-aligned.

Qualitatively there is a good correspondence between the experimental data and the model. The model captures the general features in the data, including the high field region of increasing critical current with increasing applied field and the low field region ($H < 1.4$ T) in which the critical current increases with decreasing field. However, the model predicts significantly lower critical currents (factor of ~ 5) and more hysteresis than that observed in the experiment. The latter is perhaps not surprising as we have assumed single domain dynamics in the model and likely the relaxation to the low energy magnetic state occurs via non-uniform magnetic states of the free layer.

The strongest evidence for current induced magnetization reversal at high fields comes from the experimental observation summarized in Fig. 3. Here we show MR measurements at fixed current bias. For low enough currents the spin-transfer torque cannot initiate magnetization dynamics, independent of the magnitude of the applied fields. An increase in magnetic field leads only to a more parallel alignment of the two layers. An example for this case is shown in Fig. 3a. Here the bias current I is below a threshold current $I_t \approx 26.6$ mA. The field dependence of the device resistance changes dramatically, once the bias current exceeds I_t (Fig. 3b). In this case, one can distinguish between three distinct field regions. The boundaries H_1 , H_2 and H_3 of these three regions depend on the current bias. In the first region ($H_1 < H < H_2$) an increase of the magnitude of the applied field leads again to a parallel alignment. In the second region ($H_2 < H < H_3$) precessional states become possible and a gradual and *reversible* transition from parallel to anti-parallel alignment takes place. At the boundary between the second and third region ($H = H_3$) a reversible but sharp transition from anti-parallel back to parallel configuration takes place. In the third region, where $H > H_3$, the pillar device remains in the parallel configuration. A further increase in current bias (Fig. 3c) shows that at high enough currents the high field transition from anti-parallel to parallel alignment becomes *hysteretic* whereas the low field transition from parallel to anti-parallel alignment remains reversible. The width of the hysteresis depends on the current bias and the polarity of the applied field. In general it increases with

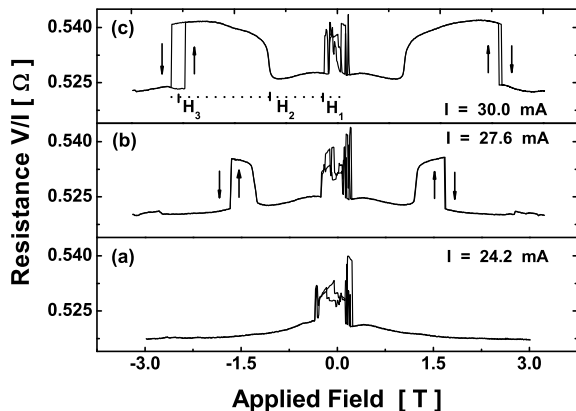


FIG. 3: (a) dV/dI versus H for fields oriented in the plane of the thin-film layer and small bias currents. The inset shows the layers sequence. (b) dV/dI versus I of the same device. The applied field is $H=2.2$ T and oriented perpendicular to the film plane. At a critical current a peak structure occurs in the dynamic resistance. The dotted line shows dV/dI at negative currents, for which the peak structure is absent.

increasing current bias.

This behavior is in sharp contrast to earlier reports [3, 6, 8]. In Ref. 8, when a high in-plane field was applied to a pillar device, a large plateau in the magnetoresistance with intermediate resistance R_{int} value ($R_{AP} > R_{int} > R_P$) was observed. The resistance plateau was attributed to a precessing spin-wave state in-between P and AP alignment. From Fig. 3 it is clear that in the field perpendicular geometry a large plateau in the magnetoresistance is absent. In comparison to point-contact experiments on magnetic multilayers and on single bulk Co layers [3, 6, 23] high bias currents in pillar devices appear to lead to a complete magnetization reversal even at high magnetic fields.

In summary, we have presented strong evidence for current induced switching in Co/Cu/Co pillar devices at high magnetic fields. In the field perpendicular geometry we have shown the existence of two distinct field regions at which a transition between parallel and anti-parallel alignment takes place. In the low field region the magnetization reverses gradually to an anti-parallel alignment through precessional states. In the high field region, at high enough current bias, a hysteretic switching of the layers takes place.

The authors gratefully acknowledge useful discussions with S. Zhang, P. M. Levy and R. Kohn. This research was supported by an NSF-FRG and by DARPA-ONR.

-
- [1] J. Slonczewski, J. Magn. Magn. Mater. **159**, L1 (1996)
 - [2] L. Berger, Phys. Rev. B **54**, 9353 (1996).
 - [3] M. Tsoi *et al.*, Phys. Rev. Lett. **80**, 4281 (1998).
 - [4] J. Z. Sun, J. Magn. Magn. Mater. **202**, 157 (1999).
 - [5] J.-E. Wegrowe *et al.*, Europhys. Lett. **45**, 626 (1999).
 - [6] M. Tsoi *et al.*, Nature **406**, 46 (2000).
 - [7] E. B. Myers *et al.*, Science **285**, 867 (1999).
 - [8] J. A. Katine *et al.*, Phys. Rev. Lett. **84**, 3149 (2000).
 - [9] J. Grollier *et al.*, Appl. Phys. Lett. **78**, 3663, (2001).
 - [10] F. J. Albert *et al.*, Appl. Phys. Lett. **77**, 3809, (2000).
 - [11] J. Grollier *et al.*, arXiv:cond-mat/0211371.
 - [12] F. J. Albert *et al.*, Phys. Rev. Lett. **89**, 226802 (2002).
 - [13] J. Z. Sun *et al.*, Appl. Phys. Lett. **81**, 2202, (2002).
 - [14] J. Z. Sun *et al.*, to be published in J. Appl. Phys. (2003).
 - [15] J. Slonczewski, J. Magn. Magn. Mater. **195**, L261 (1999).
 - [16] G. E. W. Bauer *et al.*, arXiv:cond-mat/0205453.
 - [17] M. D. Stiles and A. Zangwill, J. Appl. Phys. **91**, 6812 (2002)
 - [18] X. Waintal *et al.*, Phys. Rev. B **62**, 12317 (2000).
 - [19] A. Shpiro, P. M. Levy and S. Zhang, arXiv:cond-mat/0212045 (2002).
 - [20] J. Z. Sun *et al.*, Phys. Rev. B **62**, 570, (2000).
 - [21] Z. Li and S. Zhang, preprint (2002).
 - [22] K. Wang *et al.*, Phys. Rev. B **54**, 11965 (1996).
 - [23] Y. Ji and C.L. Chien, arXiv:cond-mat/0210116 (2002).

This figure "Figure2jpg.JPG" is available in "JPG" format from:

<http://arxiv.org/ps/cond-mat/0301324v2>